Space-Time Spreading Aided Distributed MIMO-WSNs

Indrakshi Dey , *Senior Member, IEEE*, Hemdutt Joshi , *Member, IEEE*,
and Nicola Marchetti, *Senior Member, IEEE*

Abstract—In this letter, we consider the plaguing, yet rarely handled problem of interference resulting from superposition of multiple sensor signals in time, when sent over a multiple access channel (MAC) in wireless sensor networks (WSNs). We propose space-time spreading (STS) of local sensor decisions before reporting them over a MAC to i) minimize interference and ii) reduce energy required for combating interference due to superposition of sensor decisions. Each sensor decision is encoded on appropriately indexed space-time block of fixed duration using dispersion vectors, such that a single sensor is activated over each space-time block while all the other sensors are silent. At the receive side of the reporting channel, we assume a multi-antenna decision fusion center (DFC), thereby representing a distributed multiple-input-multiple-output (MIMO) communication scenario. We formulate and compare optimum and sub-optimum fusion rules for fusing sensor decisions at the DFC to arrive at a reliable conclusion. Simulation results demonstrate gain in fusion performance with STS-aided transmission by 3 to 6 times over performance without STS.

Index Terms—Wireless sensor networks, decision fusion, space-time spreading, Internet of Things, distributed MIMO.

I. Introduction

IN TRADITIONAL WSNs, each sensor is allocated a dedicated orthogonal channel for transmitting their local observations. However, in the emerging paradigm of IoT that involves coexistence of a multitude of sensors, the bandwidth requirement increases linearly with the number of sensors [1]. Hence, in large-scale WSNs, all sensors transmit their decisions simultaneously over a MAC to a DFC that receives a superposition of the sensor decisions.

In a MAC scenario, the bandwidth requirement no longer depends on the number of sensors. However, DF in MAC is corrupted with intrinsic interference resulting from inter-sensor-element interference (ISEI) and inter-sensor-channel interference (ISCI) [2]. Interference caused by partial overlap of multiple sensor signals in time results in ISEI, while ISCI is caused by the superposition of sensor signals when sent over a MAC. Together with interference, the wireless MAC suffers from random time-varying fading and shadowing.

In order to combat fading, shadowing and interference inherent to MAC, the transmission energy required for covering a single-hop can be quite high to compensate for the signal losses incurred by the environment. But sensor nodes are energy-constrained and low-power, and high energy transmission is taxing on the battery life of the sensors. The rise in the number of IoT-based applications incorporating WSNs, has therefore increased the need for energy-efficient transmission over wireless MAC suffering from ISEI and ISCI along with fading and shadowing.

Implementing multiple antennas at the DFC is recommended in [3], [4] to improve fusion performance in deep fading and shadowing condition, thereby leveraging a 'virtual' MIMO or massive MIMO (mMIMO) channel between the sensors and the DFC. The results in [3], [4] are extended in [5] to scenarios with non-perfect CSI for both antipodal and non-antipodal signalling formats. However, MIMO and mMIMO based DF in MAC is still corrupted with ISEI and ISCI. An alternative solution is to group sensors into clusters [6], where sensors within each cluster report their observations to their cluster-head and each cluster-head reports its decision to the DFC over each time-slot. However, such a technique, though capable of minimizing co-channel interference, involves two-stage fusion and introduces extra error in the fusion process.

Orthogonality in Space-time coding (STC) aided MIMO [7]–[9] can fight interference and fading in multi-access environments, but at the cost of high encoding and decoding complexities. However, STC-aided MIMO or mMIMO based WSN is not a viable option owing to energy, bandwidth, complexity constraints and higher system knowledge (like channel parameters, sensor local decisions) requirements.

The primary contribution of this letter is to propose i) space-time spreading (STS) of sensor decisions on the transmit side to minimize interference in an energy-efficient way before receiving them over a wireless MAC and ii) fusing the decisions at multi-antenna DFC with the aim of achieving significant improvement in fusion performance in presence of deep fading and shadowing. The key idea of STS aided WSN is to map local sensor decisions on indexed space-time blocks of fixed duration by multiplying individual decision vectors with different dispersion vectors, such that each sensor transmits on a particular space-time slot when all the other sensors are silent. Since no two sensors transmit on the same space-time slot, possibility of ISEI and ISCI is almost eliminated. Moreover, no extra energy is needed to overcome interference, thereby resulting in energy-efficient interference-free transmission over large-scale WSNs at a reduced complexity. We derive two sets of sub-optimum DF techniques with reduced complexity for the received signal at the DFC consisting of a) Decode-and-fuse and b) Decode-then-fuse
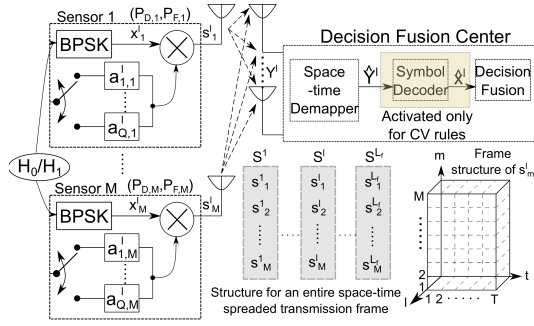
Fig. 1. ST Spreading aided WSN with distributed MIMO DF.

rules, generalizing to our set-up those introduced in [4], [10] for MIMO and mMIMO DF context. Towards this end, this letter will clarify on how distributed DF will perform in STS aided WSNs.

II. SYSTEM OVERVIEW

Fig. 1 portrays the schematic diagram for an STS-aided WSN employing M transmit sensors ($m \triangleq \{1, \ldots, M\}$) and N receive antennas at the DFC over T symbol duration over L_f space-time (ST) blocks in each transmission frame [11].

A. System Model

The sensors take a local decision autonomously based on a binary hypothesis test, $\mathcal{H}_0$ or $\mathcal{H}_1$, concerning absence and presence of a target of interest respectively. The local decision taken by the mth sensor is first mapped to a binary phase shift keyed (BPSK) symbol, $x_m^l \triangleq \{+1, -1\}$ multiplied by a T-length dispersion vector, $\mathbf{a}_{q,m}^l$, transmitted by the mth sensor in the lth time-slot to yield, $\mathbf{s}_m^l = x_m^l \mathbf{a}_{q,m}^l \in \mathbb{C}^{1 \times T}$ for ($l = 1, 2, \ldots, L_f$). Here, $\mathbf{a}_{q,m}^l = [a_{q,m,1}^l, a_{q,m,2}^l, \ldots, a_{q,m,T}^l] \in \mathbb{C}^{1 \times T}$ is the mth row of the qth ST dispersion matrix $\mathbf{A}_q^l = [\mathbf{a}_{q,1}^l, \mathbf{a}_{q,2}^l, \ldots, \mathbf{a}_{q,M}^l]^t \in \mathbb{C}^{M \times T}$ selected out of the Q ST matrices taken from the set $\{\mathbf{A}_q^l\}_{q=1}^Q$. The encoded set of sensor decisions $\mathbf{S}^l \in \mathbb{C}^{M \times T} \triangleq [\mathbf{s}_1^l, \mathbf{s}_2^l, \ldots, \mathbf{s}_M^l]^t = [x_1^l \mathbf{a}_{q,1}^l, x_2^l \mathbf{a}_{q,2}^l, \ldots, x_M^l \mathbf{a}_{q,M}^l]^t$ must include ST dispersion matrices (DMs) that satisfy the power constraint of $Tr(\mathbf{A}_q^{l\ H} \mathbf{A}_q^l) = T \ \forall \ q$ to ensure unity energy over each ST block. For ease of representation, we employ parametric system definition in terms of (M, N, T, Q) for any STS-aided WSN. It is to be noted here that STS includes the space spreading (SS) or spatial modulation-like [12] arrangement $(M, N, 1, Q = M)$ as a special case.

Example Scenario: Let us assume the DMs to be 4×4 matrices, where a single sensor out of 4 sensors over one out of 4 ST blocks is activated. Hence we have $T = M = 4$ with $Q = 1$ DM activated out of $Q = 4$, such that the activated DM, $\mathbf{A}_q^l = [1\ 0\ 0\ 0; 0\ 1\ 0\ 0; 0\ 0\ 1\ 0; 0\ 0\ 0\ 1]$. The mapping of the sensor decisions on the chosen DM can be exhibited as, Time'1', Sensor'1' $\rightarrow \mathbf{s}_1^l = [x_1^l\ 0\ 0\ 0]$, Time'2', Sensor'2' $\rightarrow \mathbf{s}_2^l = [0\ x_2^l\ 0\ 0]$, Time'3', Sensor'3' $\rightarrow \mathbf{s}_3^l = [0\ 0\ x_3^l\ 0]$ and Time'4', Sensor'4' $\rightarrow \mathbf{s}_4^l = [0\ 0\ 0\ x_4^l]$ to create the encoded set of sensor decision,

$$\mathbf{S}^l \triangleq [\mathbf{s}_1^l\ \mathbf{s}_2^l\ \mathbf{s}_3^l\ \mathbf{s}_4^l]^t = \begin{bmatrix} x_1^l & 0 & 0 & 0 \\ 0 & x_2^l & 0 & 0 \\ 0 & 0 & x_3^l & 0 \\ 0 & 0 & 0 & x_4^l \end{bmatrix}$$

B. Transmission Signal Model

Following the sensor decision mapping, the generic $N \times T$ ($n \triangleq \{1, \ldots, N\}$, $t \triangleq \{1, \ldots, T\}$) discrete-time received signal matrix at the DFC is denoted by,

$$\mathbf{Y}^l = \sqrt{\rho^l} \mathbf{G}^l \mathbf{S}^l + \mathbf{w}^l \triangleq [\mathbf{y}_1^l, \mathbf{y}_2^l, \ldots, \mathbf{y}_N^l]^t \in \mathbb{C}^{N \times T} \quad (1)$$

where $\mathbf{Y}^l$, $\mathbf{G}^l \in \mathbb{C}^{N \times M}$ and $\mathbf{w}^l \sim \mathcal{N}_{\mathbb{C}}(\mathbf{0}_{N \times T}, \sigma_w^{l\ 2} \mathbf{I}_{N \times T})^{[1],[2]}$ are the received signal vector, the channel matrix and the noise vector respectively. The constant ρ^l denotes the energy spent by any of the sensors during the reporting phase and $\mathbf{G}^l$ includes all the samples of the channel impulse response (CIR) between the sensors and the DFC over the lth ST block.

C. Channel Model

The generic channel coefficient vector $g_{n,m}^l$ is expressed as $g_{n,m}^l = \sqrt{\lambda_m} h_{n,m}^l$, where λ_m models the geometric attenuation and shadow fading and remains constant over n and l. Based on these assumptions, we have $\mathbf{G}^l = \mathbf{H}^l \sqrt{\mathbf{D}}$ where $\mathbf{G}^l \in \mathbb{C}^{N \times M}$ denotes the matrix of the generic channel coefficients, $\mathbf{H}^l \in \mathbb{C}^{N \times M}$ denotes the matrix of the fast fading coefficients and $\mathbf{D} \in \mathbb{C}^{M \times M}$ is a diagonal matrix with $d_{m,m} = \lambda_m$.

D. Reception Signal Model

At the receiver, i.e. the DFC, by applying the vectorial stacking operation $vec()$ to the received signal block $\mathbf{Y}^l$ at the ST de-mapper, we arrive at the linearized equivalent received signal model formulated as,

$$\hat{\mathbf{Y}}^l = \sqrt{\rho^l} \hat{\mathbf{G}}^l \hat{\mathcal{A}}^l \hat{\mathbf{K}}^l + \hat{\mathbf{w}}^l = vec(\mathbf{Y}^l) \in \mathbb{C}^{NT \times 1} \quad (2)$$

where $\hat{\mathbf{G}}^l = \mathbf{I}_g \otimes \mathbf{G}^l \in \mathbb{C}^{NT \times MT}$ (where $\mathbf{I}_g = \mathbf{I}_{T \times T}$) is the estimated channel matrix [3] and $\otimes$ is the Kronecker product, $\hat{\mathbf{w}}^l = vec(\mathbf{w}^l) \in \mathbb{C}^{NT \times 1}$, $\hat{\mathcal{A}}^l = \mathbf{I}_a \otimes \mathbf{A}^l \in \mathbb{C}^{MT \times MQ}$ (where $\mathbf{I}_a = \mathbf{I}_{M \times M}$ and $\mathbf{A}^l \triangleq [\mathbf{A}_1^l, \mathbf{A}_2^l, \ldots, \mathbf{A}_Q^l]^t$) and $\hat{\mathbf{K}}^l = vec(\mathbf{K}^l) \triangleq vec([\mathbf{0}, \ldots, \mathbf{0}, \mathbf{x}^l, \mathbf{0}, \ldots, \mathbf{0}]) \in \mathbb{C}^{MQ \times 1}$ and $\mathbf{x}^l = [x_1^l, x_2^l, \ldots, x_M^l]^t \in \mathbb{C}^{M \times 1}$ is the transmit vector.

E. Decision Fusion

The DFC is in charge of providing a reliable decision (i.e. $\mathcal{H}^1, \ldots, \mathcal{H}^{L_f}$) on the basis of the superimposed received decisions taken locally by the sensors independently over each ST block (i.e. $\hat{\mathbf{Y}}^1, \ldots, \hat{\mathbf{Y}}^{L_f}$) by employing optimum or sub-optimum fusion rules. In this letter, we will consider and compare two types of fusion rules to arrive at a reliable choice depending on the scenario.

The first set of rules (Decode-and-fuse) aims at concluding on the presence or absence of the target directly from the

---

[1]The noise vector also accounts for different levels of channel state information (CSI) estimation error, where the estimated channel on the receiver side is contaminated by additive Gaussian noise.

[2]$(\cdot)^t$ denotes transpose, $\mathbb{R}(\cdot)$, $\mathbb{E}\{\cdot\}$, $\mathbb{V}\{\cdot\}$, $\angle(\cdot)$, $(\cdot)^\dagger$, $|| \cdot ||$, $p(\cdot)$ and $P(\cdot)$ represents real-part, expectation, variance, phase, conjugate transpose, Frobenius norm operators, probability density function and probability mass function respectively; $\mathcal{N}(\mu, \Sigma)$ denote normal distribution with mean μ and co-variance matrix Σ.

[3]The DFC estimates the CSI, where half of the coherence interval of $2T$ is used for training to estimate the channel and establish the frequency and timing synchronization. It is worth mentioning that the linearized sensor-DFC system model contains M non-zero symbol components in $\hat{\mathbf{K}}^l$ given by $\mathbf{x}^l$.

received signal without processing the transmit signal; the optimum (opt) test statistics for which is given by,

$$\mathbf{\Gamma}_{\text{opt}}^l \approx \ln \left[\frac{\sum_{\mathbf{x}^l} \exp\left(-\frac{\left\|\hat{\mathbf{Y}}^l - \sqrt{\rho^l}(\hat{\mathbf{G}}^l \hat{\mathcal{A}}_q^l)\mathbf{x}^l\right\|^2}{\sigma_w^2}\right) P\left(\mathbf{x}^l \mid \mathcal{H}_1^l\right)}{\sum_{\mathbf{x}^l} \exp\left(-\frac{\|\hat{\mathbf{Y}}^2 - \sqrt{\rho^l}(\hat{\mathbf{G}}^l \hat{\mathcal{A}}_q^l)\mathbf{x}^l\|^2}{\sigma_w^l}\right) P\left(\mathbf{x}^l \mid \mathcal{H}_0^l\right)} \right] \tag{3}$$

assuming conditional independence of $\hat{\mathbf{Y}}^l$ from $\mathcal{H}_j^l$, given $\mathbf{x}^l$, and $\hat{\mathbf{G}}^l \in \mathbb{C}^{NT \times MT}$, $\hat{\mathcal{A}}_q^l \in \mathbb{C}^{MT \times M}$ and $\mathbf{x}^l \in \mathbb{C}^{M \times 1}$. The second set of fusion rules (Decode-then-fuse) firstly estimates the transmit signal from the received signal and then arrives at a global decision based on the estimated transmit signal vector $\bar{\mathbf{x}}^l$. The test statistics using Chair-Varshney (CV) rule for noiseless channel is given by,

$$\mathbf{\Gamma}_{\text{CV}}^l = \xi^l \ln\left(\frac{P(\mathbf{x}^l|\mathcal{H}_1)}{P(\mathbf{x}^l|\mathcal{H}_0)}\right) + \left(1 - \xi^l\right) \ln\left(\frac{1 - P(\mathbf{x}^l|\mathcal{H}_1)}{1 - P(\mathbf{x}^l|\mathcal{H}_0)}\right) \tag{4}$$

where $\xi^l = \frac{\bar{\mathbf{x}}^l + 1}{2}$. In this case, the symbol decoder block in Fig. 1 at the DFC computes $\bar{\mathbf{x}}^l$.

F. Fusion Rules

In the first group of fusion rules, we consider three suboptimum rules, Maximal Ratio Combining (MRC), modified MRC (mMRC) and Widely Linear (WL) rules; the test statistics of which are given by (assuming identical sensor performances),

$$\mathbf{\Gamma}_{\text{MRC}}^l \propto \mathbb{R}\{\mathbf{1}_M^t (\hat{\mathbf{G}}^l \hat{\mathcal{A}}_q^l)^\dagger \hat{\mathbf{Y}}^l\}$$
$$\mathbf{\Gamma}_{\text{mMRC}}^l \propto \mathbb{R}\{\mathbf{1}_M^t (\hat{\mathbf{G}}^l \hat{\mathcal{A}}_q^l)^\dagger (\mathbf{D}_g^l)^{-1} \hat{\mathbf{Y}}^l\}$$
$$\mathbf{\Gamma}_{i,\text{WL}}^l \triangleq \left(\frac{\mathbf{\Sigma}_{\underline{\hat{\mathbf{Y}}}^l|\hat{\mathbf{G}}^l \hat{\mathcal{A}}_q^l, \mathcal{H}_i^l}^{-1} \underline{\hat{\mathbf{G}}^l} \hat{\mathcal{A}}_q^l \boldsymbol{\mu}_i^l}{\left\|\mathbf{\Sigma}_{\underline{\hat{\mathbf{Y}}}^l|\hat{\mathbf{G}}^l \hat{\mathcal{A}}_q^l, \mathcal{H}_i^l}^{-1} \underline{\hat{\mathbf{G}}^l} \hat{\mathcal{A}}_q^l \boldsymbol{\mu}_i^l\right\|}\right)^\dagger \underline{\hat{\mathbf{Y}}}^l \tag{5}$$

where $\mathbf{D}_g^l = \frac{1}{N}(\hat{\mathbf{G}}^l \hat{\mathcal{A}}_q^l)^\dagger (\hat{\mathbf{G}}^l \hat{\mathcal{A}}_q^l)$ is a diagonal matrix for $N \gg M$, $\mathbf{\Sigma}_{\underline{\hat{\mathbf{Y}}}^l|\hat{\mathbf{G}}^l \hat{\mathcal{A}}_q^l, \mathcal{H}_i^l}^{-1} = \left(\rho^l \underline{\hat{\mathbf{G}}^l} \hat{\mathcal{A}}_q^l \mathbf{\Sigma}_{\mathbf{x}^l|\mathcal{H}_i^l} (\underline{\hat{\mathbf{G}}^l} \hat{\mathcal{A}}_q^l)^\dagger + \sigma_{w,l}^2 \mathbf{I}_{2N}\right)^4$ is chosen such that the deflection measure $\mathcal{D}_i(\cdot)$ is maximized, $\mathcal{D}_0(\cdot)$ correspond to the normal and and $\mathcal{D}_1(\cdot)$ corresponds to the modified deflection [13], $\boldsymbol{\mu}_i^l \triangleq 2\left[(P_{D,1}^l - P_{F,1}^l) \ldots (P_{D,M}^l - P_{F,M}^l)\right]^t$, $\mathbf{P}_{D,m}^l \triangleq P(\hat{\mathbf{K}}_m^l = [0, \ldots, 0, x_m^l = 1, 0, \ldots, 0]^t|\mathcal{H}_1)$ and $\mathbf{P}_{F,m}^l \triangleq P(\hat{\mathbf{K}}_m^l = [0, \ldots, 0, x_m^l = 1, 0, \ldots, 0]^t|\mathcal{H}_0)$ respectively, the probabilities of detection and false alarm of the mth sensor on the lth ST block.

In the second group, we consider three different decoders to estimate $\bar{\mathbf{x}}^l$ from $\hat{\mathbf{Y}}^l$; the global decision $\hat{\mathcal{H}}$ is taken on the basis of $\bar{\mathbf{x}}^l$, which includes maximum likelihood (ML), zero forcing (ZF) and minimum mean squared error (MMSE) detector given by,

$$\bar{\mathbf{x}}_{\text{ML}}^l = \overset{\text{argmin}}{\mathbf{x}^l} \left\|\hat{\mathbf{Y}}^l - \sqrt{\rho^l}(\hat{\mathbf{G}}^l \hat{\mathcal{A}}_q^l)\mathbf{x}^l\right\|^2$$
$$\bar{\mathbf{x}}_{\text{MMSE}}^l = (\hat{\mathbf{G}}^l \hat{\mathcal{A}}_q^l)^\dagger \left(\left(\mathbf{D}_g^l + \frac{\sigma_w^l^2}{\sqrt{\rho^l}}\mathbf{I}_M\right)^{-1}\right)^\dagger \hat{\mathbf{Y}}^l$$
$$\bar{\mathbf{x}}_{\text{ZF}}^l = (\hat{\mathbf{G}}^l \hat{\mathcal{A}}_q^l)^\dagger \left((\mathbf{D}_g^l)^{-1}\right)^\dagger \hat{\mathbf{Y}}^l \tag{6}$$

Once $\bar{\mathbf{x}}^l$ is obtained, we plug it in the CV-rule to obtain the test statistics for CV-ML and CV-MMSE rules.

III. PERFORMANCE METRICS

In this section, some insights on the probability of detection or false-alarm, design criteria for the DMs and the complexity associated with different fusion rules when employed in an STS-aided WSN are provided.

A. Performance Measures

Combining the decisions from all the M sensors independently over each ST block, we can arrive at the total probabilities $P_{D_0,\text{rule}}^l (\triangleq \Pr\{\Gamma_{\text{rule}}^l > \gamma^l | \hat{\mathbf{G}}^l \hat{\mathcal{A}}_q^l, \mathcal{H}_1^l\})$ and $P_{F_0,\text{rule}}^l (\triangleq \Pr\{\Gamma_{\text{rule}}^l > \gamma^l | \hat{\mathbf{G}}^l \hat{\mathcal{A}}_q^l, \mathcal{H}_0^l\})$ respectively for the presented network and each fusion rule, where Γ_{rule}^l is the generic test statistics and γ^l is the threshold with which the test statistics for each rule is compared. Assuming $\mathbb{E}\{\mathbf{x}^l|\mathcal{H}_0^l\} \triangleq (2 P_F^l - 1)\mathbf{I}_M$ and $\mathbb{E}\{(\mathbf{x}^l - \mathbb{E}\{\mathbf{x}^l|\mathcal{H}_0^l\})(\mathbf{x}^l - \mathbb{E}\{\mathbf{x}^l|\mathcal{H}_0^l\})^t|\mathcal{H}_0^l\} \triangleq [1 - (2 P_F^l - 1)^2]\mathbf{I}_M$, we can compute $P_{F_0,\text{rule}}^l$ for the formulated fusion rules as below. Alternatively, it is to be noted here that, we can also compute $P_{D_0,\text{rule}}^l$ by assuming, $\mathbb{E}\{\mathbf{x}^l|\mathcal{H}_1^l\} \triangleq (2 P_D^l - 1)\mathbf{I}_M$ and $\mathbb{E}\{(\mathbf{x}^l - \mathbb{E}\{\mathbf{x}^l|\mathcal{H}_1^l\})(\mathbf{x}^l - \mathbb{E}\{\mathbf{x}^l|\mathcal{H}_1^l\})^t|\mathcal{H}_1^l\} \triangleq [1 - (2 P_D^l - 1)^2]\mathbf{I}_M$.

Assuming $P(\mathbf{Y}^l|\hat{\mathbf{G}}^l \hat{\mathcal{A}}_q^l, \mathcal{H}_j^l)$ follow Gaussian mixture distribution, $\Gamma_{j,\text{rule}}^l|\hat{\mathbf{G}}^l \hat{\mathcal{A}}_q^l, \mathcal{H}_j^l$ is also distributed according to Gaussian mixture model. Using Gaussian moment matching [14], we have, $\Gamma_{j,\text{rule}}^l|\hat{\mathbf{G}}^l \hat{\mathcal{A}}_q^l, \mathcal{H}_j^l \overset{\text{approx}}{\sim} \mathcal{N}\left(\mathbb{E}\{\Gamma_{j,\text{rule}}^l|\hat{\mathbf{G}}^l \hat{\mathcal{A}}_q^l, \mathcal{H}_j^l\}, \mathbb{V}\{\Gamma_{j,\text{rule}}^l|\hat{\mathbf{G}}^l \hat{\mathcal{A}}_q^l, \mathcal{H}_j^l\}\right)$. Under simplifying assumptions of $\mathbb{E}\{\mathbf{x}^l|\mathcal{H}_0^l\} \triangleq (2 P_F^l - 1)\mathbf{1}_M = \delta^l$, we arrive at the low signal-to-interference-plus-noise ratio (SINR) approximation for $P_{F_0,\text{rule}}^l$ as,

$$P_{F_0,\text{rule}}^l = \lim_{N \to \infty} \mathcal{Q}\left(\frac{\gamma^l - \frac{\mathbb{E}\{\Gamma_{j,\text{rule}}^l|\hat{\mathbf{G}}^l \hat{\mathcal{A}}_q^l, \mathbf{x}^l\}}{\sqrt{\mathbb{V}\{\Gamma_{j,\text{rule}}^l|\hat{\mathbf{G}}^l \hat{\mathcal{A}}_q^l, \mathbf{x}^l\}}}}{\sqrt{1/2((1 - \delta^{l^2})M + \sigma_w^{l^2})}}\right). \tag{7}$$

where $\mathcal{Q}(\cdot)$ is used to denote the complementary cumulative distribution function (CCDF). Since at low SINR, the components of the Gaussian mixture gets concentrated within a certain region, we need to evaluate the mean and variance of $\Gamma_{j,\text{rule}}^l$ for each fusion rule summarized in Table I with $\mathbf{V}_j^l \triangleq \mathbf{I}_M - \left(\frac{1 + \sigma_w^{l^2}}{2\mathbf{D}_g^l \rho^l N \sqrt{N} \mathbf{\Sigma}_{\mathbf{x}^l|\mathcal{H}_j^l}^{-1}}\right)^{-1}$ and $\mathbf{B}_g^l = \left(\mathbf{D}_g^l + \frac{\sigma_w^{l^2}}{\sqrt{\rho^l}}\mathbf{I}_M\right)^{-1}$. Putting the values from Table I in (7), we can arrive at $P_{F_0,\text{rule}}^l$ for each fusion rule.

B. Design Criteria for DMs

For the performance analysis, we have chosen $Q = M = T$. Accordingly, we choose our DM based on random search following the steps:

- Randomly generate Q unitary dispersion matrix set $\{\mathbf{A}_q^l\}_{q=1}^Q$ using Gaussian distribution, such that $Tr(\mathbf{A}_q^{l^H} \mathbf{A}_q^l) = T \; \forall \; q$.

---

[4] $\underline{\mathbf{u}}$ (resp. $\underline{\mathbf{U}}$) denotes the augmented vector (resp. matrix) of $\mathbf{u}$ (resp. $\mathbf{U}$) i.e., $\underline{\mathbf{u}} \triangleq [\mathbf{u}^t \; \mathbf{u}^\dagger]^t$ (resp. $\underline{\mathbf{U}} \triangleq [\mathbf{U}^t \; \mathbf{U}^\dagger]^t$)

TABLE I
MEAN AND VARIANCE OF $\mathbf{\Gamma}_{j,\text{RULE}}^l$ FOR THE CONSIDERED FUSION RULES

Fusion Rule	$\mathbb{E}\{\mathbf{\Gamma}_{j,\text{rule}}^l|\hat{\mathbf{G}}^l\hat{\mathcal{A}}_q^l,\mathbf{x}^l\}$	$\mathbb{V}\{\mathbf{\Gamma}_{j,\text{rule}}^l|\hat{\mathbf{G}}^l\hat{\mathcal{A}}_q^l,\mathbf{x}^l\}$
MRC	$\sqrt{\rho^l}\mathbb{R}\{(\mathbf{1}_M)^t\mathbf{D}_g^l\mathbf{x}^l\}$	$\frac{\sigma_w^{l^2}}{2N}\|(\mathbf{1}_M)^t\mathbf{D}_g^l\mathbf{1}_M\|$
mMRC	$\sqrt{\rho^l}\mathbb{R}\{(\mathbf{1}_M)^t\mathbf{x}^l\}$	$\frac{\sigma_w^{l^2}}{2N}\|(\mathbf{1}_M)^t\mathbf{D}_g^l\mathbf{1}_M\|$
WL	$\sqrt{\rho^l}(\mu_j^l)^t\mathbf{V}_j^l\mathbf{D}_g^l\mathbf{x}^l$	$\frac{\sigma_w^{l^2}}{2N}\|(\mu_j^l\mathbf{V}_j^l)^t\mathbf{D}_g^l\mu_j^l\mathbf{V}_j^l\|$
CV-ML	$\sqrt{\rho^l}\mathbf{D}_g^l\mathbf{x}^l$	$\frac{\sigma_w^{l^2}}{2N}\|\mathbf{D}_g^l\|$
CV-MMSE	$\sqrt{\rho^l}\mathbf{B}_g^l\mathbf{D}_g^l\mathbf{x}^l$	$\frac{\sigma_w^{l^2}}{2N}\|(\mathbf{B}_g^l)^t\mathbf{D}_g^l\mathbf{B}_g^l\|$
CV-ZF	$\sqrt{\rho^l}\mathbf{x}^l$	$\frac{\sigma_w^{l^2}}{2N}\|(\mathbf{D}_g^l)^{-1}\|$

TABLE II
COMPLEXITY ANALYSIS FOR THE CONSIDERED FUSION RULES

Fusion Rule	Complexity for each realization of $\mathbf{x}^l$
Optimum	$\mathcal{O}(NMQT2^{MQ})$
(m)MRC, WL	$\mathcal{O}(NT)$
CV-ML, CV-MMSE, CV-ZF	$\mathcal{O}(NMQT)$

- The matrix generation is repeated for 10 times.
- For each of the 10 sets of $\{\mathbf{A}_q^l\}_{q=1}^Q$, calculate the corresponding $P_{D_0,\text{Opt}}^l((\gamma^l,\hat{\mathbf{G}}^l\hat{\mathcal{A}}_q^l))$

$$= 1 - \lim_{N\to\infty} \mathcal{Q}\left(\frac{\gamma^l - \frac{N\sqrt{2\rho^l}\mathbf{D}_g^l\{P(\mathbf{x}^l|\mathcal{H}_1^l)/P(\mathbf{x}^l|\mathcal{H}_0^l)\}}{\sigma_w^{l^2}\|\mathbf{D}_g^l\{P(\mathbf{x}^l|\mathcal{H}_1^l)/P(\mathbf{x}^l|\mathcal{H}_0^l)\}\|}}{\sqrt{1/2((1-\delta^{l^2})M+\sigma_w^{l^2})}}\right). \quad (8)$$

- Out of the sets of $\{\mathbf{A}_q^l\}_{q=1}^Q$, the set exhibiting the maximum $P_{D_0,\text{Opt}}^l((\gamma^l,\hat{\mathbf{G}}^l\hat{\mathcal{A}}_q^l))$ is chosen for simulating performance.

C. Complexity Analysis

In Table II, we compare the computational complexity of the formulated rules, for each new $\mathbf{x}^l$ transmitted, in terms of the Landau notation $\mathcal{O}(\cdot)$, i.e. the order of complexity.

IV. PERFORMANCE ANALYSIS

We simulate performance of a (M,N,T,Q) STS-aided WSN, where M sensors are randomly deployed and uniformly distributed in a circular annulus around the DFC with radii $\phi_{\max} = 1000$ m and $\phi_{\min} = 100$ m. We assume $Q = T = M$ to exploit full diversity order and enhance opportunistic network throughput. The ST spreaded local decisions of the sensors are transmitted over a log-normal shadowed and Rayleigh block faded channel, such that $\mathbf{h}_{n,m}^l \sim \mathcal{N}_{\mathbb{C}}(0,\text{diag}(\mathcal{B}_m^l))$, where $\lambda_m^l = \psi_m(\frac{\phi_{\min}}{\phi_m})^\eta$, $\mathcal{B}_m^l = (\beta_m^l(0),\ldots,\beta_m^l(T-1))^t$ is the channel power delay profile with $\sum_{\tau=0}^{T-1}\beta_m^l(\tau) = 1$, $10\log_{10}(\psi_m) \sim \mathcal{N}(\mu_\lambda \text{ dB}, \sigma_\lambda^2 \text{ dB})$, η is the pathloss exponent and ϕ_m is the distance of the mth sensor to the DFC. We also assume $\rho^l = 1/\sqrt{N}$ and independently and identically distributed (iid) decisions with $(P_D^l,P_F^l) = (0.5,0.05)$.

In Fig. 2 and Fig. 3, we present the Receiver Operating Characteristics (ROC) of all the fusion rules for two different configurations of WSNs, a) fully-loaded MIMO set-up $(M = 8, N = 8)$ and b) virtual mMIMO set-up $(M = 10, N = 100)$. We simulate performance of the formulated fusion rules over a MAC with pathloss exponent, η of 2, experiencing moderate shadowing, $(\mu_\lambda,\sigma_\lambda) = (4,2)$ dB.
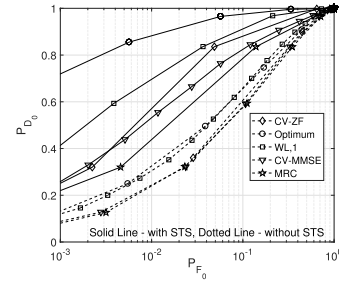
Fig. 2. Comparative ROC (P_{D_0} v/s P_{F_0}) of different fusion rules in $(8,8,8,8)$ STS-aided WSNs with that in WSNs without STS-aided decision transmission over a fixed SINR of 15 dB. Both the sensors and DFC are deployed in a variety of indoor environments.
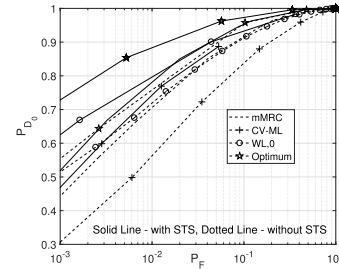
Fig. 3. Comparative ROC (P_{D_0} v/s P_{F_0}) of different fusion rules in $(10,100,10,10)$ STS-aided WSNs with that in WSNs without STS-aided decision transmission over a fixed SINR of 15 dB. Both the sensors and DFC are deployed in a variety of indoor environments.

The above-mentioned parameters are representative of a variety of indoor environments. For the two network set-ups, STS aided sensor decision transmission offers significant improvement in performance over that without STS. Each fusion rule gains in performance from a minimum of 3 times (MRC) to a maximum of 6 times (Opt.) in case of fully-loaded MIMO, and a maximum of 8-9 times (Opt.) to a minimum of 3-4 times (CV-ML) in case of virtual mMIMO set-up. For both the set-ups, MRC (mMRC for mMIMO case) and CV-ML perform worst respectively, as corroborated in [4], [10].

In Fig. 4, we establish the validity of our derived expressions for performance evaluation of the formulated fusion rules in Section III-A, by comparing simulated and analytical performances. The analytical performances match closely with and in many cases, almost identically to the simulated performances. The reason can be attributed to the fact that the channel samples for the analytical results are generated using the same channel model used for generating the simulation results.

In Fig. 5, we plot P_{D_0} of the presented fusion rules as a function of N under $P_{F_0} \leq 0.01$; we depict the case $M = 4$. Performance of all fusion rules improves with the increase in N, except MRC, however reaches saturation depending on the SINR and the chosen fusion rule. Some rules like CV-MMSE, and CV-ZF ($N > 40$) proceeds to saturation faster than other rules like WL,0 ($N > 90$). It is also evident that MRC performs worse than any other fusion rule, as MRC does not exploit STS aided local sensor performance at the decoding stage like WL, CV-MMSE or CV-ZF. Indeed, the probability of detection with MRC is dependent only on the channel statistics.

In Fig. 6, we demonstrate P_{D_0} of the presented fusion rules as a function of $(SINR)_{dB}$, where the SINR measure includes channel noise, varying levels of CSI estimation errors
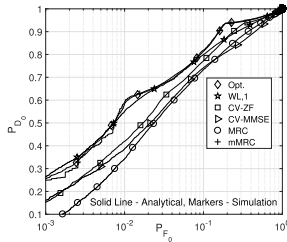
Fig. 4. Comparative analytical and simulation performance for different fusion rules in $(4, 20, 4, 4)$ STS-aided WSNs over a fixed SINR of 15 dB. Both the sensors and DFC are deployed in a variety of indoor environments.
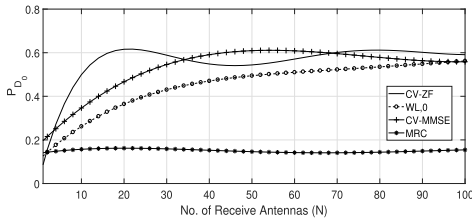
Fig. 5. Variation in probability of detection of different fusion rules with changing N (P_{D_0} v/s N) for $(4, N, 8, 8)$ STS-aided WSNs over a fixed SINR of 15 dB and $P_{F_0}^l = 0.01$. The sensors are deployed in a tunnel-like environment.
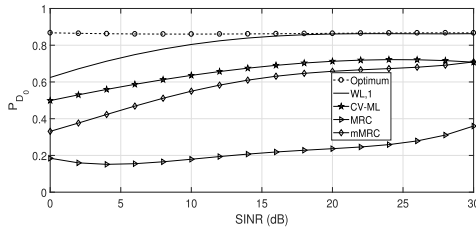
Fig. 6. Comparative probability of detection performance (P_{D_0} v/s SINR(dB)) for different fusion rules in an $(8, 32, 8, 8)$ STS-aided WSN where outdoor sensors communicate with an indoor DFC.

and interference. In this case, $N = 3, M = Q = T = 8$ and $\eta = 5$ and $\mu_\lambda = 4$ dB, a representative condition of outdoor sensors communicating with indoor DFC. CV-MMSE, CV-ZF and WL,1 rules approach the optimal performance at moderate to high SINRs. However, MRC, mMRC and CV-ML rules fail to achieve optimal performance even at high SINRs, as opposed to the observations made in [15]. It has been demonstrated in [16], that for $T > 1$, diversity increases but at the cost of reliability for STSK modulated systems. For $Q > 1$, throughput increases but at the cost of degraded bit error rate (BER). Here, we have chosen $T = Q = M$ for STS thereby sacrificing reliability of system knowledge (like CSI statistics, statistics of sensor decision vectors) and lower probability of error for the sake of gain in diversity and network throughput. It can be broadly concluded that CV-ML performs poorly in any network scenario and propagation condition as the CV-ML statistics is dependent on the channel SINR which is kept fixed for Figs. 2, 3, and 5.

V. CONCLUSION

In order to strike a flexible balance between interference minimization and energy efficiency in massive WSNs for IoT applications, we conceive the novel idea of ST spreading the local sensor decisions before transmission in a WSN. The resultant network will not only benefit from improvement in opportunistic throughput but also from ISCI and ISEI

free transmission in a densely deployed scenario. The STS scheme used can be modified depending on the chosen Q and T to include Spatial Modulation (SM) [12], Space-Shift Keying (SSK) [17] and Space-Time Shift Keying (STSK) [16] arrangements. However, using different values for Q, T, M will involve multiple information symbols for carrying sensing decisions, an interesting generalization which we leave for our future work. Our presented simulation results demonstrate the potential of STS-aided WSN in outperforming the conventional MIMO and mMIMO based WSN arrangements. Motivated by this observation, in future, we plan to extend our results under different conditions of dispersion matrix optimization, multi-slot decision transmission and correlated sensor observations in sensing performance.

REFERENCES

[1] A. Argyriou and Ö. Alay, "Distributed estimation in wireless sensor networks with an interference canceling fusion center," *IEEE Trans. Wireless Commun.*, vol. 15, no. 3, pp. 2205–2214, Nov. 2015.

[2] V. Rao, R. Prasad, T. Prabhakar, C. Sarkar, M. Koppal, and I. Niemegeers, "Understanding and improving the performance of constructive interference using destructive interference in WSNs," *IEEE/ACM Trans. Netw.*, vol. 27, no. 2, pp. 505–517, Feb. 2019.

[3] I. Dey, M. M. Butt, and N. Marchetti, "Throughput analysis for virtual MIMO WSNs over measured MIMO channels," *IEEE Trans. Instrum. Meas.*, vol. 68, no. 1, pp. 297–299, Oct. 2019.

[4] D. Ciuonzo, G. Romano, and P. S. Rossi, "Channel-aware decision fusion in distributed MIMO wireless sensor networks: Decode-and-fuse vs. Decode-then-fuse," *IEEE Trans. Wireless Commun.*, vol. 11, no. 8, pp. 2976–2985, Aug. 2012.

[5] A. Chawla, A. Patel, A. K. Jagannatham, and P. K. Varshney, "Distributed detection in massive MIMO wireless sensor networks under perfect and imperfect CSI," *IEEE Trans. Signal Process.*, vol. 67, no. 15, pp. 4055–4068, Jun. 2019.

[6] S. Althunibat and R. Mesleh, "Index modulation for cluster-based wireless sensor networks," *IEEE Trans. Veh. Technol.*, vol. 67, no. 8, pp. 6943–6950, Aug. 2018.

[7] S. M. Alamouti, "A simple transmit diversity technique for wireless communications," *IEEE J. Sel. Areas Commun.*, vol. SAC-16, no. 8, pp. 1451–1458, Oct. 1988.

[8] P. W. Wolniansky, G. J. Foschini, G. D. Golden, and R. A. Valenzuela, "V-BLAST: An architecture for realizing very high data rates over the rich-scattering wireless channel," in *Proc. URSI Int. Symp. Signals, Syst., Electron.*, Oct. 1998, pp. 295–300.

[9] B. Hassibi and B. M. Hochwald, "High-rate codes that are linear in space and time," *IEEE Trans. Inf. Theory*, vol. 48, no. 7, pp. 1804–1824, Jul. 2002.

[10] D. Ciuonzo, P. S. Rossi, and S. Dey, "Massive MIMO channel-aware decision fusion," *IEEE Trans. Signal Process.*, vol. 63, no. 3, pp. 604–619, Feb. 2015.

[11] I. Dey *et al.*, "Decision fusion in space-time spreading aided distributed MIMO WSNs," 2020, *arXiv:2005.08011*. [Online]. Available: http://arxiv.org/abs/2005.08011

[12] R. Y. Mesleh, H. Haas, S. Sinanovic, C. W. Ahn, and S. Yun, "Spatial modulation," *IEEE Trans. Veh. Technol.*, vol. 57, no. 4, pp. 2228–2241, Jul. 2008.

[13] Z. Quan, S. Cui, and A. H. Sayed, "Optimal linear cooperation for spectrum sensing in cognitive radio networks," *IEEE J. Sel. Topics Signal Process.*, vol. 2, no. 1, pp. 28–40, Feb. 2008.

[14] Y. Bar-Shalom, T. Kirubarajan, and X. R. Li, *Estimation with Applications to Tracking and Navigation: Theory Algorithms and Software*. Hoboken, NJ, USA: Wiley, 2004.

[15] I. Dey, P. S. Rossi, M. M. Butt, and N. Marchetti, "Virtual MIMO wireless sensor networks: Propagation measurements and fusion performance," *IEEE Trans. Antennas Propag.*, vol. 67, no. 8, pp. 5555–5568, May 2019.

[16] S. Sugiura, S. Chen, and L. Hanzo, "Coherent and differential space-time shift keying: A dispersion matrix approach," *IEEE Trans. Commun.*, vol. 58, no. 11, pp. 3219–3230, Nov. 2010.

[17] J. Jeganathan, A. Ghrayeb, L. Szczecinski, and A. Ceron, "Space shift keying modulation for MIMO channels," *IEEE Trans. Wireless Commun.*, vol. 8, no. 7, pp. 3692–3703, Jul. 2009.